Modeling and Simulation of Multiple Nonlinearities Using TLM

Venkata Dinavahi, *Member, IEEE*

***Abstract*— This paper introduces a new application of the Transmission Line Modeling (TLM) method for the modeling and simulation of systems containing multiple nonlinear elements. Originally proposed for the analysis of low-power electronic devices and for the solution of finite element problems, TLM has the unique ability to decouple nonlinear element(s) from the network and from each other so that they can be solved individually using Newton-Raphson (N-R). This is the key which allows for greater accuracy, stability, faster convergence and lower computational burden. A detailed case study of a nonlinear bridge circuit is presented to illustrate the advantages of the TLM method vis-à-vis the conventional Newton method. It is shown that the TLM method offers significant advantages in terms of convergence, accuracy and computational speed.**

***Index Terms*— Nonlinear circuits, Modeling, Newton-Raphson method, Simulation.**

I. Introduction

NONLINEAR elements are ubiquitous in power systems. Whether they are magnetic, arcing, or power electronic in nature, nonlinearities have a significant impact on the system voltages and currents, and therefore require accurate and efficient techniques of analysis under transient and steady-state conditions. Conventional techniques used for the inclusion of nonlinear elements in EMTP-type programs include the Compensation Method and the Network Equivalent's Method [1]. Both these methods derive their effectiveness from separating the linear part of the network from the non-linear part, and then using an iterative technique based on Newton-Raphson (N-R) to arrive at the solution. In the Compensation Method, compensation theorem in conjunction with triangular factorization of nodal equations is used to separate the nonlinear element from the linear part of the network. While in the Network Equivalent's method, the N-R iterative process is confined to the nodes where the nonlinear element is connected by reducing the linear part of the network to an equivalent. However, one of the fundamental limitations of these methods is that in the presence of multiple nonlinear elements in the network, a simultaneous solution of nonlinear equations using N-R is required, which puts a restriction on the convergence, accuracy and efficiency of the overall solution. This is because the full Jacobian matrix has to be dealt with in every iteration. Another limitation of the above methods is that proper initial conditions are required to ensure convergence to the correct AC steady-state solution. The speed of convergence is slower if the simulation is started from zero initial conditions.

An alternate approach- Transmission Line Modeling (TLM) -for modeling lumped networks containing both linear and nonlinear elements was first proposed by Johns and O'Brien [2] for the analysis of transistor circuits. They showed that the formulation resulting from using the TLM method is similar to the one obtained by using an implicit numerical integration scheme such as the Trapezoidal rule, thereby making the TLM model unconditionally stable. TLM also offered the advantage of physically interpreting the numerical errors as parasitic inductance and capacitance. Later Hui and Christopoulos [3]–[5], in a series of articles, developed a comprehensive formulation for a TLM based discrete transform technique for solving linear integro-differential equations and extended its application to model power electronics. More recently, the TLM technique has been used to solve finite element problems [6], [7].

This paper proposes a new application of the TLM method for the transient simulation of systems with multiple nonlinear elements. The main advantage of using the TLM method to address this problem is that it effectively decouples the nonlinear elements from each other as well as from the linear part of the network. Thus, the nonlinear elements can be solved individually, rather than simultaneously, using N-R iteration. Furthermore, using the TLM technique a large network can be split into smaller sub-networks which can be solved faster than the original network. This could be a very promising application for real-time digital simulation. The basic principle of the TLM method is described in Section II where the TLM models for lumped linear and nonlinear elements are presented and the solution process is explained. A detailed case study of a nonlinear bridge circuit is presented in Section III. The performance of the TLM method, in terms of convergence, accuracy and CPU time requirement, is compared with that of the conventional N-R method and the results are presented in Section IV. Finally, Section V presents the conclusions of the study.

II. Basic TLM Methodology

A. TLM Models for Lumped Linear Elements

The surge or characteristic impedance of a loss-less transmission line is given as $Z_o = \sqrt{L/C}$. Depending on the values of L and C, the line can be made predominantly inductive or capacitive.

The TLM model for a linear inductor (Fig. 1(B)) consists of a short-circuited loss-less line with surge impedance $Z_L =$

Financial support from the Natural Science and Engineering Research Council of Canada (NSERC) is gratefully acknowledged.

V. Dinavahi is with the Department of Electrical & Computer Engineering, University of Alberta, Edmonton, AB T6G 2V4, Canada (e-mail: dinavahi@ece.ualberta.ca).

Presented at the International Conference on Power Systems Transients (IPST'05) in Montreal, Canada on June 19-23, 2005
Paper No. IPST05 - 032

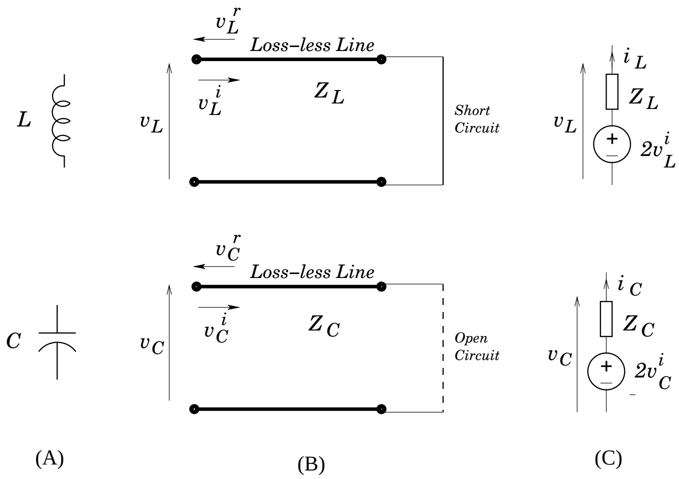

Fig. 1. (A) Linear element, (B) TLM Model (C) Thévénin Equivalent

$\Delta t/2L$, where $\Delta ti/2$ is the travel time of the voltage or current waves on the line. For calculating those waves numerically, it also becomes the time-step of the transient simulation. From the Thévénin equivalent shown in Fig. 1(C), the voltage across the inductor at the n^{th} time-step is given as:

$$ {}_n v_L = Z_L \cdot {}_n i_L + 2 \cdot {}_n v_L^i \tag{1} $$

where ${}_n v_L^i$ is the incident voltage pulse and ${}_n i_L$ is the inductor current, at the n^{th} time-step. From transmission line theory ${}_n v_L$ is also equal to the sum of the incident pulse ${}_n v_L^i$ and the reflected pulse ${}_n v_L^r$, i.e.,

$$ {}_n v_L = {}_n v_L^i + {}_n v_L^r \tag{2} $$

For the short-circuit at the far end the reflection coefficient is -1. Thus, the reflected pulse ${}_n v_L^r$ will become inverted and act as the incident pulse for the next time-step, i.e.,

$$ {}_{n+1} v_L^i = - {}_n v_L^r = {}_n v_L^i - {}_n v_L \tag{3} $$

Similar voltage equations can be developed for linear coupled inductors.

The TLM model for a linear capacitor (Fig. 1(B)) consists of a open-circuited loss-less line with surge impedance $Z_C = 2C/\Delta t$. From the Thévénin equivalent in Fig. 1(C), the voltage across the capacitor at the n^{th} time-step can be expressed as:

$$ {}_n v_C = Z_C \cdot {}_n i_C + 2 \cdot {}_n v_C^i \tag{4} $$
$$ = {}_n v_C^i + {}_n v_C^r \tag{5} $$

For the open-circuit at the far end the reflection coefficient is +1. Thus, the voltage pulse will be reflected without inversion and becomes the incident pulse for the next time-step, i.e.,

$$ {}_{n+1} v_C^i = + {}_n v_C^r = {}_n v_C - {}_n v_C^i \tag{6} $$

The TLM model for a linear resistor R will be simply:

$$ {}_n v_R = R \cdot {}_n i_R \tag{7} $$

It can be easily shown that the TLM models for L and C are identical to discrete-time companion models obtained using the Trapezoidal rule. Furthermore, it can be shown that the TLM capacitor model has a small associated inductance of $L_C = \Delta t^2/4C$ and that the TLM inductor model has a small associated capacitance of $C_L = \Delta t^2/4L$. These associated elements L_C and C_L are also present in the models obtained using Trapezoidal rule, but they are usually treated as modeling errors. If Δt is large, these errors are large, and if Δt is small, the errors become small as well. A physical interpretation of these errors can be derived by recognizing that real inductors do have stray capacitances and that real capacitors also have stray inductances. The parasitic components introduced by the TLM models are similar to stray components in real inductors and capacitors. Thus, the TLM method allows us to estimate the modeling errors in terms of parasitic inductances and capacitances and choose a proper value of Δt that might reduce those errors.

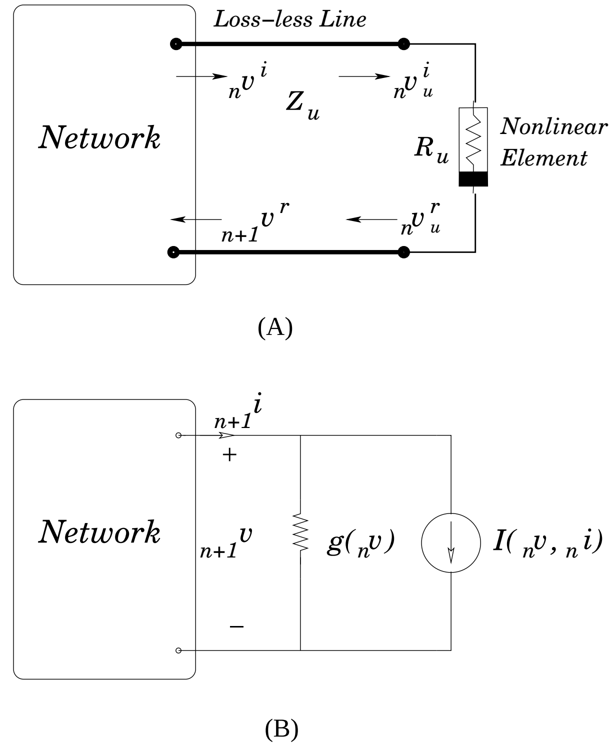

Fig. 2. (A) TLM model of a nonlinear element (B) Associated N-R discrete circuit

B. TLM Model for a Non-linear Element

Fig. 2(A) shows a nonlinear element R_u connected by a loss-less transmission line, with surge impedance Z_u and travel time $\Delta t/2$, to the network. At the n^{th} iteration, the network launches a pulse ${}_n v^i$ into the nonlinear branch, which becomes an incident pulses v_u^i on the nonlinear element at $\Delta t/2$. A reflected pulse produced by the nonlinear element v_u^r becomes the next incident pulse ${}_{n+1} v^r$ on the network at Δt. Let the nonlinear element be described as follows:

$$ i_u = f_u(v_u) \tag{8} $$

The incident and reflected voltage pulses at the nonlinear element are related to the current pulse through the following equation:

$$i_u = \frac{1}{Z_u}\left(v_u^i - v_u^r\right) \tag{9}$$

Also, from tranmission line theory,

$$v_u = v_u^i + v_u^r \tag{10}$$

Substituting (9) and (10) into (8), the reflected pulse from the nonlinear element can be obtained as follows:

$$v_u^i - v_u^r = Z_u * f\left(v_u^i + v_u^r\right) \tag{11}$$

(11) is a single nonlinear equation which is independent of the rest of the network, and therefore it can be solved individually by N-R. Similar equations can be developed for other nonlinear elements in the network. Fig. 2(B) shows the discrete circuit associated with N-R solution for the nonlinear element R_u, where

$$g({}_nv) = \left(\frac{\mathrm{d}i_u}{\mathrm{d}v_u}\right)_{v={}_nv} \quad \text{and} \quad I({}_nv,\ {}_ni) = {}_ni - g\ {}_nv \tag{12}$$

From (12) it can be seen that the conductance g across the terminals of the network changes with every iteration of N-R. This has the effect of changing the network nodal admittance matrix at every iteration. Alternately, if the nonlinearity is expressed as:

$$v_u = f_u(i_u) \tag{13}$$

Then the reflected pulse from the nonlinear element can be obtained as:

$$v_u^i + v_u^r = f_u\left(\frac{v_u^i + v_u^r}{Z_u}\right) \tag{14}$$

The choice of the surge impedance Z_u is arbitrary and its value influences the speed of convergence of the solution. If Z_u is chosen such that it matches the final value of R_u at convergence, then the reflected wave from the nonlinear element is zero, and the solution is obtained in one iteration. Of course, since this matched value is not known *a priori*, reflections or iterations must continue until convergence to the final solution.

C. TLM Network Solution

Let $\mathcal{N}$ be a general network to which inductors, capacitors and nonlinear elements are connected externally to ports. Each of these three groups of elements are represented using TLM models. Assuming that all other elements such as linear resistors, independent voltage and current sources and any linear controlled sources, are inside $\mathcal{N}$, the TLM procedure operates by transmitting pulses along the transmission lines. The overall model is discrete in time since the pulses remain constant in magnitude during their transit back and forth on the lines with travel time $\Delta t/2$.

Assume that the sources within $\mathcal{N}$ are emitting pulses corresponding the same time period Δt. At time $t = 0$ the sources will inject pulses out of the ports of $\mathcal{N}$. These pulses will travel along the lines, be reflected and travel back towards $\mathcal{N}$. At time $t = \Delta t$ the pulses will be incident upon $\mathcal{N}$ and will scatter into all the ports of $\mathcal{N}$. These reflected pulses together with new injections from the sources are again launched into the lines and the process repeats. For a synchronous operation all lines have the same delay Δt.

Let the incident and reflected pulses at time $t = \Delta t$ be given as:

$$\begin{aligned} {}_n\mathbf{v}^i &= [\,{}_nv_1^i\ {}_nv_2^i \ldots\ {}_nv_k^i]^T & (15)\\ {}_n\mathbf{v}^r &= [\,{}_nv_1^r\ {}_nv_2^r \ldots\ {}_nv_k^r]^T & (16)\end{aligned}$$

Now, pulses are only incident upon and reflected into branches which are also ports. Therefore, the values of incident and reflected pulses are set to be zero on branches which are not ports. Thus for p ports, ${}_nv_q^i = 0$ and ${}_nv_q^r = 0$ for $q > p$. Let

$$\begin{aligned} \mathbf{I} &= [I_1\ I_2\ \ldots\ I_k]^T & (17)\\ \mathbf{E} &= [E_1\ E_2\ \ldots\ E_k]^T & (18)\end{aligned}$$

be the independent current sources in branches and voltage sources across branches respectively. Also, let $\mathbf{Y_b}$ be the branch admittance matrix. For the first p branches this matrix will contain diagonal entries corresponding to the surge impedances of the transmission lines. The remaining matrix elements ($p+1$ to k) correspond to linear resistors and linear controlled sources of the network.

The equivalent nodal source vector $\boldsymbol{\mathcal{I}}$ at the n^{th} time-step is given by

$${}_n\boldsymbol{\mathcal{I}} = \mathbf{A}(\mathbf{I} - \mathbf{Y}_b\mathbf{E} - 2\mathbf{Y}_b\,{}_n\mathbf{v}^i) \tag{19}$$

where $\mathbf{A}$ is the reduced incidence matrix. The nodal admittance matrix is given as:

$$\mathbf{Y} = \mathbf{A}\ \mathbf{Y}_b\ \mathbf{A}^T \tag{20}$$

The network solution in terms of the nodal voltages ${}_n\mathbf{v}$ at the n^{th} time-step is obtained by solving

$${}_n\mathbf{v} = \mathbf{Y}^{-1}\,{}_n\boldsymbol{\mathcal{I}} \tag{21}$$

Then, the reflected pulses are calculated from the fact that the sum of the incident and reflected voltage pulses at a node must equal the nodal voltage. Thus,

$${}_n\mathbf{v}^r = \mathbf{A}^T\,{}_n\mathbf{v} - {}_n\mathbf{v}^i \tag{22}$$

The reflected pulses now travel back on the lines to the same ports, or they are transmitted to adjacent networks. Thus,

$${}_{n+1}\mathbf{v}^i = \mathbf{C}\,{}_n\mathbf{v}^r \tag{23}$$

where $\mathbf{C}$ is the connection matrix with elements of 1 to describe how the lines are connected.

The TLM solution repeats equations (19), (21)-(23)at every time-step. If there are multiple nonlinear elements connected to the network, the TLM procedure advances to the next time-step only when the individual solutions for all nonlinear elements have converged, thereby maintaining synchronism. For a simultaneous N-R solution, $\mathbf{Y}^{-1}$ in (21) must be calculated at every iteration. However, in the TLM solution, $\mathbf{Y}$ remains unchanged from iteration to iteration since its entries are the Z_u's of the transmission lines and other linear elements; hence, $\mathbf{Y}^{-1}$ needs to be calculated only once at the beginning of the simulation.

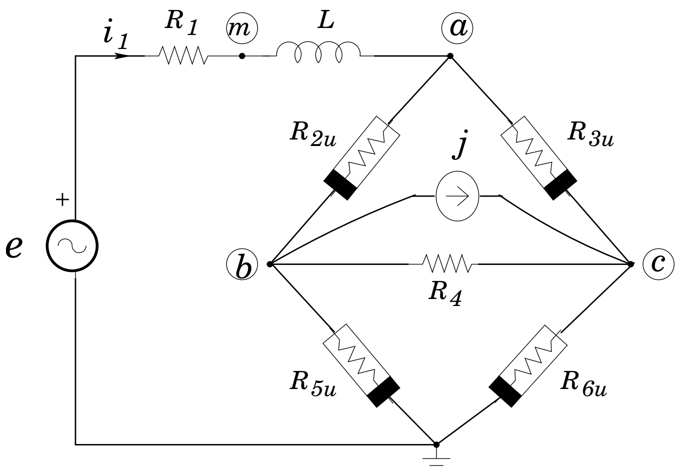

Fig. 3. Nonlinear Resistor Bridge

III. Case Study - Nonlinear Bridge Circuit

Fig. 3 shows a bridge circuit [8] containing four nonlinear resistors ($R_{ku},\ k = 2,3,5,6$), two linear resistors (R_1 and R_4), one linear inductor L and two independent sources ($e(t)$ and $j(t)$). Resistors R_{3u} and R_{5u} are characterized by the equation $i_u = I_s\left[e^{v_u/V_T} - 1\right]$ whereas the resistors R_{2u} and R_{6u} are characterized by $i_u = -I_s\left[e^{-v_u/V_T} - 1\right]$. With such characteristics the operation of the bridge resembles that of a full-wave diode rectifier. This circuit, whose parameters are given in Table I has been used to compare the performance of the full N-R method with that of the TLM method. The comparison of the two methods was made on the criteria of convergence (number of iterations), accuracy (RMS error in fundamental currents and voltages) and CPU time requirement under two starting conditions: (1) zero initial conditions and (2) matched initial conditions. The two methods were coded in MATLAB and executed on a AMD Athlon XP 1.8 GHz processor running Linux.

A. Full N-R Solution

The Full N-R problem is to find $\mathbf{x} \in \mathbb{R}^3$ such that

$$\mathbf{f}(\mathbf{x}) = \mathbf{0}, \quad \mathbf{f} : \mathbb{R}^3 \mapsto \mathbb{R}^3 \tag{24}$$

with

$$\mathbf{x} = [v_a\ v_b\ v_c]^T \text{ and } \mathbf{f} = [f_1\ f_2\ f_3]^T \tag{25}$$

where the nonlinear functions of the bridge obtained using nodal analysis are given as:

$$\begin{aligned} f_1 &= I_s(e^{\frac{v_b - v_a}{V_T}} - 1) - I_s(e^{\frac{v_a - v_c}{V_T}} - 1) \\ &\quad + \frac{\Delta t}{2L}(v_m - v_a) + I_L(t - \Delta t) \end{aligned} \tag{26}$$

$$\begin{aligned} f_2 &= -R_4 I_s(e^{\frac{v_b - v_a}{V_T}} - 1) - R_4 I_s(e^{\frac{v_b}{V_T}} - 1) \\ &\quad + (v_c - v_b) - R_4 j(t) \end{aligned} \tag{27}$$

$$\begin{aligned} f_3 &= R_4 I_s(e^{\frac{v_c - v_a}{V_T}} - 1) + R_4 I_s(e^{\frac{v_c}{V_T}} - 1) \\ &\quad - (v_c - v_b) + R_4 j(t) \end{aligned} \tag{28}$$

TABLE I
Circuit Data for the Case Study

Parameter	Value
R_1,R_4	$1\ k\Omega$
L	$1\ mH$
$e(t)$	$10\ \cos(\omega t)$
$j(t)$	$10^{-3}\cos(\omega t)$
I_s	10^{-14} A
V_T	$26\ mV$
ω	$377\ rad/s$
Z_L,Z_{ku}	500Ω

where

$$v_m = \frac{1}{\frac{1}{R_1} + \frac{\Delta t}{2L}}\left[\frac{e}{R_1} + \frac{v_a \Delta t}{2L} - I_L(t - \Delta t)\right] \tag{29}$$

and

$$I_L(t - \Delta t) = \frac{\Delta t}{2L}\left[v_m(t - \Delta t) - v_a(t - \Delta t)\right]. \tag{30}$$

The solution of (24) is given as:

$$\mathbf{x}^{k+1} = \mathbf{x}^k - \mathbf{J}^{-1}\mathbf{f}(\mathbf{x}^k) \tag{31}$$

where $\mathbf{J} = \left(\frac{d\mathbf{f}}{d\mathbf{x}}\right)_{\mathbf{x}^k}$ is the Jacobian. The convergence criteria, for the Full N-R iteration, are as follows:

$$\parallel \mathbf{x}^{k+1} - \mathbf{x}^k \parallel < \epsilon_x \text{ and } \parallel \mathbf{f}\left(\mathbf{x}^{k+1}\right) \parallel < \epsilon_f. \tag{32}$$

with ϵ_x and ϵ_f set at 10^{-5}.

B. TLM Solution

The TLM model for the nonlinear bridge is obtained by replacing L and R_{ku} ($k = 2,3,5,6$) by their individual TLM models and subsequently by their Thévénin equivalent's. The surge impedances for the lines are Z_L for the inductor and Z_{ku} ($k = 2,3,5,6$) for the nonlinear resistors. At each time-step the TLM solution executes (19), (21)-(23), where

$${}_n\mathbf{v}^i = [{}_nv_L^i\ {}_nv_{2u}^i\ {}_nv_{3u}^i\ {}_nv_{5u}^i\ {}_nv_{6u}^i]^T \tag{33}$$

$$\mathbf{A} = \begin{bmatrix} -1 & 0 & 0 & 0 & 0 \\ 1 & -1 & -1 & 0 & 0 \\ 0 & 1 & 0 & -1 & 0 \\ 0 & 0 & 1 & 0 & -1 \end{bmatrix} \tag{34}$$

$${}_n\boldsymbol{\mathcal{I}} = \begin{bmatrix} \frac{e(t)}{R_1} - \frac{v_L^i}{Z_L} \\ \frac{2v_L^i}{Z_L} - \frac{2v_{2u}^i}{Z_{2u}} - \frac{2v_{3u}^i}{Z_{3u}} \\ \frac{2v_{2u}^i}{Z_{2u}} - \frac{2v_{5u}^i}{Z_{5u}} - j(t) \\ \frac{2v_{3u}^i}{Z_{3u}} - \frac{2v_{6u}^i}{Z_{6u}} - j(t) \end{bmatrix} \tag{35}$$

and

$$\mathbf{C} = diag\,[-1\ 1\ 1\ 1\ 1\ ]. \tag{36}$$

In addition, within every time-step, the reflected pulses ${}_nv_{ku}^r$, ($k = 2,3,5,6$) from the nonlinear resistors are obtained by solving the following four equations independently using N-R:

$${}_{n+1}v_{ku}^i - {}_nv_{ku}^r = \pm Z_{ku} I_s\left(e^{\pm\frac{\left({}_{n+1}v_{ku}^i + {}_nv_{ku}^r\right)}{V_T}} - 1\right) \tag{37}$$

The convergence criteria for the TLM solution are the same as in (32).

IV. Results and Discussion

A. Comparison of Convergence, Accuracy and Execution Time

Under DC conditions with $E = 10V$, $j = 1mA$ and zero initial conditions, the TLM method converged within 3 iterations to the final solution of $[v_a\ v_b\ v_c]^T = [6.15\ 0.69\ 5.45]^T$ with an absolute error tolerance of 10^{-5}, whereas the Full N-R method failed to converge to the specified tolerance. If Z_L and $Z_{ku}(k = 2, 3, 5, 6)$ are set to 467Ω, instead of 500Ω as shown in Table I then the TLM solution converged in one iteration.

Under AC steady-state conditions, Figures 4(A) and 4(B) show the percentage RMS error in the voltage $v_o(= v_c - v_b)$ and CPU time, for a simulation of 0.03s, for the two methods starting with zero initial conditions, as the simulation time step Δt is varied from $5\mu s$ to $600\mu s$. The high error and high CPU time of the Full N-R method is obvious from these figures; the y-axis is plotted in log scale to underscore the large difference in values for the two methods. Furthermore, in Fig. 4(A) discontinuities can be observed at certain points on the curve for the Full N-R method; these points denote the time-steps where the method did not converge. The TLM method, on the other hand, showed no convergence problems at any time-step. The full N-R method failed to converge beyond $\Delta t = 200\mu s$ whereas the TLM was convergent all the way up to $\Delta t = 600\mu s$.

Figures 5(A) and 5(B) show the percentage RMS error in v_o and CPU time for the two methods starting with initial conditions $[v_a\ v_b\ v_c]^T = [6\ 1\ 5]^T$. The full N-R method's error started increasing over 5% around $\Delta t = 10\ \mu s$, however, the TLM method's error stayed less than 3% up to $\Delta t = 600\ \mu s$. The large difference in error in the two methods can be seen from Fig. 5(A). The CPU time requirement for the full N-R method under matched initial conditions was found to be fairly close (Fig. 5(B)) to that of the TLM method.

B. Comparison of Time-domain Results

Figures 6, 7 and 8 show the simulation results of i_1, v_a and v_o of the bridge, for the two methods using two different time steps $\Delta t = 5\mu s$ and $\Delta t = 100\mu s$, starting from zero initial conditions. At $\Delta t = 100\mu s$, the full N-R method (Figures 6(A), 7(A) and 8(A)) start off is not very impressive and it is even prone to divergence, as shown by the spike near $t = 0.005s$. Also using the Full N-R method, even though the wave-shape of the curves for $\Delta t = 100\mu s$ is similar to those for $\Delta t = 5\mu s$, there is still a significant steady-state error. Using the TLM method (Figures 6(B), 7(B) and 8(B)) the results for the two time-steps are almost coincident with a very small error in steady-state.

Fig. 9 shows the detail of $i(t)$ for the Full N-R method and the TLM method, when the simulations were started with matched initial conditions. For the Full N-R method (Fig. 9(A)) numerical oscillations can be noticed at $\Delta t = 100\mu s$, while for the TLM method (Fig. 9(B)) no such oscillations are noticeable. The above time-domain results were verified using SPICE and PSCAD/EMTDC using detailed device models.

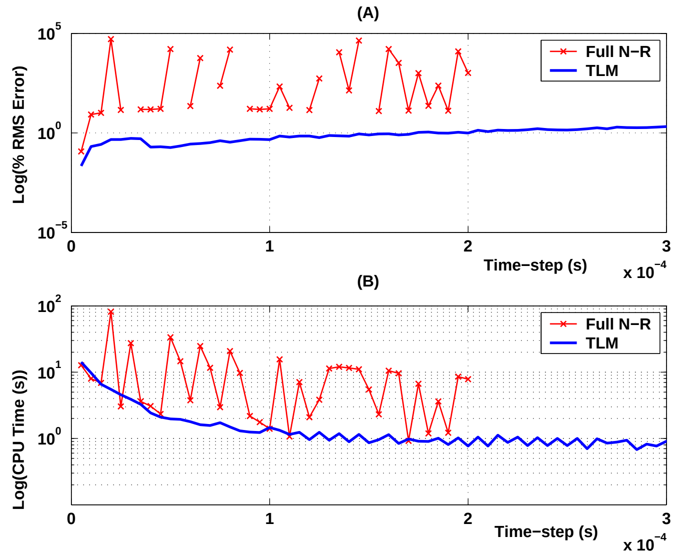

Fig. 4. Comparison of performance of the Full N-R method and the TLM method starting with *zero* initial conditions for: (A) % RMS error in v_o (B) CPU time (s).

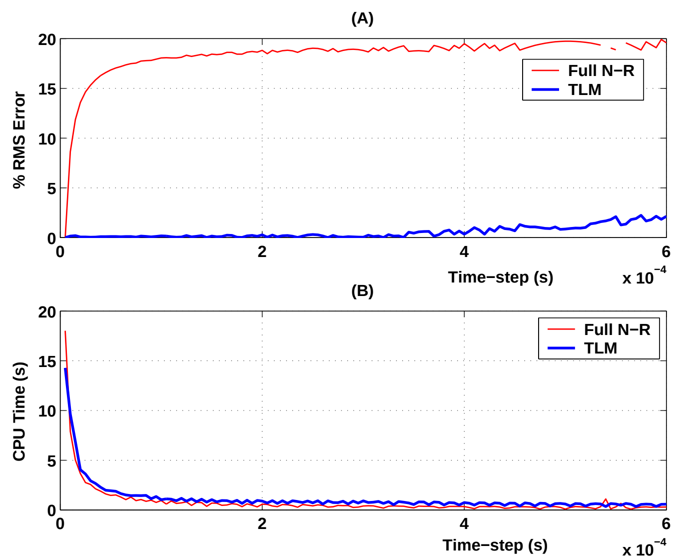

Fig. 5. Comparison of performance of the Full N-R method and the TLM method starting with *matched* initial conditions for: (A) % RMS error in v_o (B) CPU time (s).

V. Conclusions

This paper presented the application of the TLM method for the modeling and simulation of systems containing multiple nonlinearities. The TLM method is a stable and accurate modeling method which offers numerous advantages over the conventional N-R method of simultaneously solving nonlinear equations for such systems. Among its benefits are faster convergence, higher accuracy and lesser CPU time requirement compared to the Full N-R method. As such, one of the promising applications of the TLM method is for real-time digital simulation.

References

[1] H. W. Dommel, "Nonlinear and time-varying elements in digital simula-

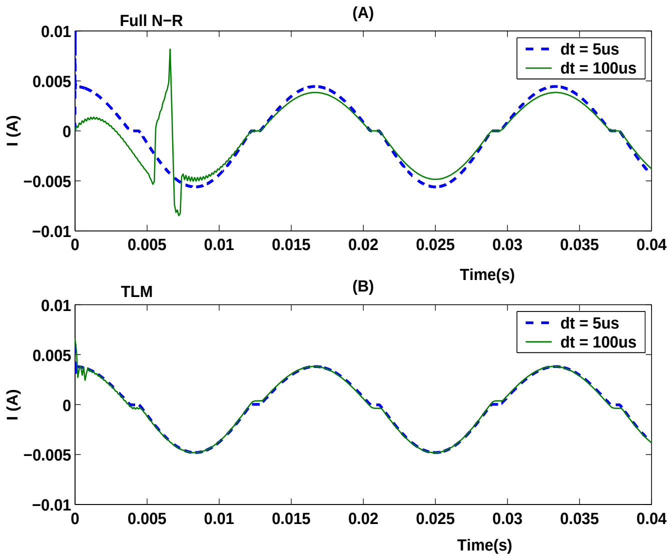

Fig. 6. Simulation results for $i(t)$ with $\Delta t = 5\mu s$ and $\Delta t = 100\mu s$ starting with *zero* initial conditions for: (A) Full N-R method, (B) TLM method.

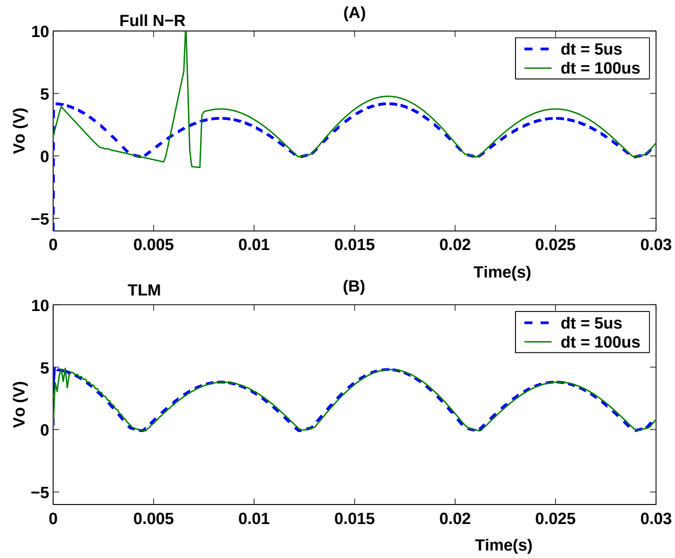

Fig. 8. Simulation results for $v_o(t)$ with $\Delta t = 5\mu s$ and $\Delta t = 100\mu s$ starting with *zero* initial conditions for: (A) Full N-R method, (B) TLM method.

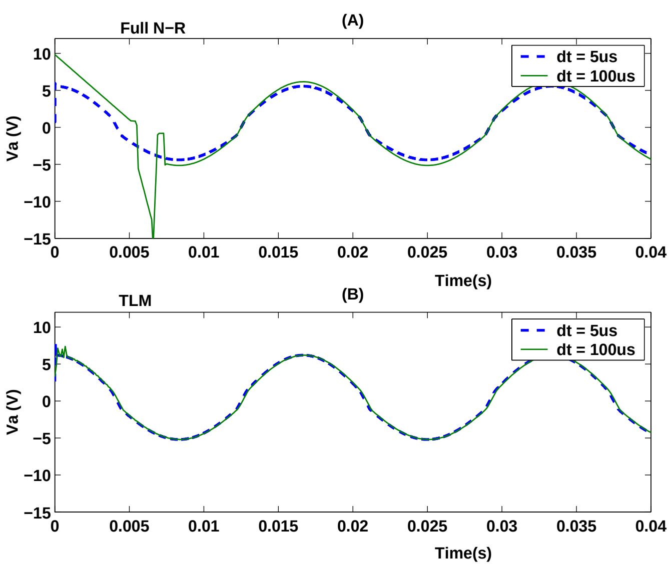

Fig. 7. Simulation results for $v_a(t)$ with $\Delta t = 5\mu s$ and $\Delta t = 100\mu s$ starting with *zero* initial conditions for: (A) Full N-R method, (B) TLM method.

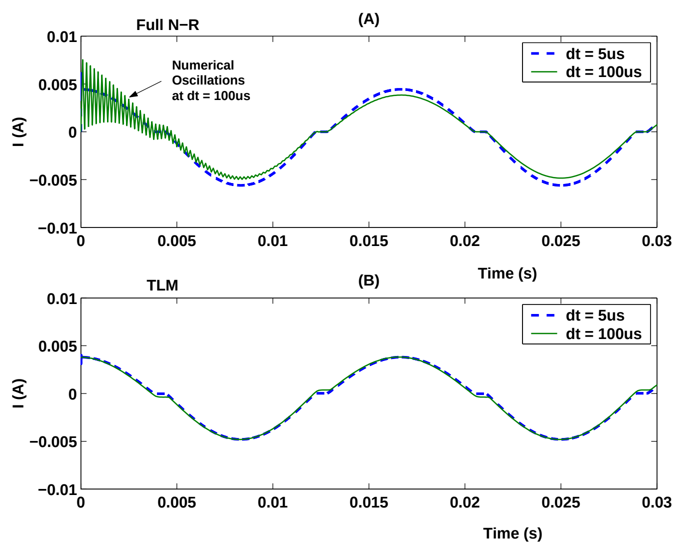

Fig. 9. Simulation results for $i_1(t)$ with $\Delta t = 5\mu s$ and $\Delta t = 100\mu s$ starting with *matched* initial conditions for: (A) Full N-R method, (B) TLM method.

tion of electromagnetic transients", *IEEE Transactions on Power Apparatus and Systems*, Vol. 90, June 1971, 2561-2567.

[2] P. B. Johns, M. O'Brien, "Use of transmission-line method to solve nonlinear lumped networks", *The Radio and Electronic Engineer*, Vol. 50, No. 1/2, January 1980, pp. 59-70.

[3] S. Y. R. Hui, C. Christopoulos, "Discrete transform technique for solving coupled integro-differential equations in digital computers ", *IEE Proceedings-A*, Vol. 138, No. 5, September 1991, pp. 273-280.

[4] S. Y. R. Hui, C. Christopoulos, "Discrete transform technique for solving nonlinear circuits and equations", *IEE Proceedings-A*, Vol. 139, No. 6, November 1992, pp. 321-328.

[5] S. Y. R. Hui, C. Christopoulos, "Modeling nonlinear power electronic circuits with the transmission-line modeling technique", *IEEE Transactions on Power Electronics*, Vol. 10, No. 1, January 1995, pp. 48-54.

[6] J. Lobry, J. Trecat, C. Broche, "The transmission line modeling method as a new iterative technique in nonlinear magnetostatics", *IEEE Transactions on Magetics*, Vol. 32, No. 2, January 1996, pp. 559-566.

[7] O. Deblecker, J. Lobry, C. Broche, "Use of transmission-line modeling method in FEM for solution of nonlinear eddy-current problems", *IEE Proceedings- Science, Measurement, Technology*, Vol. 145, No. 1, January 1998, pp. 31-38.

[8] L. O. Chua, P. Lin, *Computer Aided Analysis of Electronic Circuits: Algorithms and Computational Techniques*, Prentice-Hall, Inc., 1975.

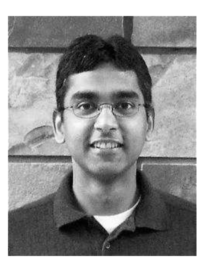

Venkata Dinavahi received the B.Eng. degree in Electrical Engineering from Nagpur University, India, in 1993, the M.Tech. degree from the Indian Institute of Technology, Kanpur, India, in 1996, and the Ph.D. degree in Electrical and Computer Engineering from the University of Toronto, Toronto, ON, Canada, in 2000. Presently, he is an Assistant Professor at the University of Alberta, Edmonton, AB, Canada. His research interests include electromagnetic transient analysis, power electronics, and real-time digital simulation and control.